Satellite imagery strategies for mapping site resonance periods at fine spacial scale

Valentin Schindelholz, Aya Cheaib, Emeline Maufroy, Cécile Cornou, Erwan Pathier, Antoine Schlupp

18TH WORLD CONFERENCE ON EARTHQUAKE ENGINEERING
WCEE2024
MILAN

MILAN, ITALY
30TH JUNE - 5TH JULY 2024
www.wcee2024.it

SATELLITE IMAGERY STRATEGIES FOR MAPPING SITE RESONANCE PERIODS AT FINE SPATIAL SCALE

V. Schindelholz[1], A. Cheaib[1], E. Maufroy[1], C. Cornou[1], E. Pathier[1] & A. Schlupp[2]

[1] ISTerre, University Grenoble Alpes, Grenoble, France, valentin.schindelholz@univ-grenoble-alpes.fr

[2] ITES, University of Strasbourg, Strasbourg, France

Abstract: *Seismic waves emitted during an earthquake are characterized by their type and propagation velocity. The velocity of shear waves (V_S) at the near-surface varies from 1000 m/s to less than 50 m/s, depending on the soil characteristics. The presence of poorly-rigid geological deposits can lead to important seismic ground-motion amplifications called site effects. Site effects can make earthquakes much more aggressive to buildings, resulting in significantly increased damage. The site effects can be characterized by several proxies such as V_{S30}, soil resonance period, surface geology and geotechnical parameters. The resonance period is one of the most relevant proxies as it accounts for the vibrational properties of the whole soil column. However, measuring resonance periods at fine spatial scale over wide areas with classical methods such as the H/V method requires a lot of measurement points which is a tedious task. As both the resonance period and the compaction rate of the sedimentary cover increase with sediment thickness and site softness, our study aims at investigating the relationship between the resonance period and the subsidence rate obtained by satellite imagery in France. We propose an innovative methodology that takes advantage of satellite SAR Interferometry time series analysis, providing subsidence rates at millimetric precision. We base our study on the Grenoble valley (southeastern France) where numerous geophysical and geological data collected over the last 25 years are available: bedrock depth map, V_{S30} map, S-wave velocity profiles, hundreds of resonance period measurements, hundreds of geotechnical and geological drillings, levelling measurements, SAR time series. Subsidence rates are compared to the various available geophysical and geological data related to near-surface and deep soil characteristics. The subsidence rate measured in the Grenoble valley is mostly caused by the compaction of the stiff and thick sediments due to natural (input of sedimentary materials on the surface) and anthropogenic (urbanization) overloading. Our analysis outlines that subsidence rates are linearly correlated with both the resonance periods and the depth of the seismic bedrock, which indicates the ability of satellite imagery to provide resonance periods at a very fine spatial scale.*

1. Introduction

When shear seismic waves propagating through the Earth's crust reach the near-surface domain, their velocity V_S can vary from 1000 m/s to less than 50 m/s. Due to the resonance of *S*-waves caused by strong impedance contrasts, poorly-rigid surface deposits can cause large ground-motion amplification, the later called sedimentary site effect. These site effects are well observed in sedimentary basins, where multiple recordings show that the seismic signal is amplified both in amplitude and duration (Bard et al., 1988; Graves et al., 1998; Frankel et al., 2002; Pratt et al., 2003; Maufroy et al., 2017). Because sedimentary basins are also areas prone to human development, high density cities are often built in regions where sedimentary amplification can occur.

In the past years, an effort has been done to incorporate site effects to seismic-hazard regulatory estimates. For example, the current European legislation, within the Eurocode 8, and some ground-motion models use the V_{S30} parameter (time-averaged shear waves velocity down to a depth of 30 m) as a criterion to classify the rigidity of the soil and to give an estimated value of the amplification (European Commission Joint Research Centre, 2012).

However, multiple issues arise with the use of this simple parameter. To account for the spatial variability of the ground motion, it is preferable to get a high-resolution mapping of V_{S30}. But retrieving V_{S30} at a fine spatial scale is rather expensive as it requires in-situ investigations which are not done systematically in every site (Cultrera et al. 2021). In the past years, proxies have been proposed to obtain estimates of V_{S30} over wide regional areas. Wald and Allen (2007) and Allen and Wald (2009) proposed to use the slope of the topography and the surface geology as a proxy to V_{S30}. Despite the large use of this proxy, in particular for Shakemaps calculation (Wald et al. 1999; Worden et al. 2010; Worden et al. 2020), recent publications tend to criticize the use of V_{S30} as the sole parameter to represent site effects, as it does not take into account the whole thickness of the soil column. It seems that the use of the resonance frequency of soils (f_0) is accurate in complement to V_{S30} to be accountable for the sedimentary amplification (Cadet, 2008; Luzi et al., 2011; Derras et al. 2017; Zhu et al., 2020). However, to get regional maps of f_0 at fine spatial scale is the same issue as for V_{S30}, because retrieving f_0 also requires in-situ geophysical measurements. Some studies (Michel et al.,2011; Albano et al., 2016) suggest that the subsidence rate in alluvial valleys is correlated with f_0 and the bedrock depth below the sediments (H_{bed}). We investigate the potential of this correlation in the city of Grenoble, France, where all required data were already collected in previous studies. Our objective is to evaluate the existence of linear correlations between the subsidence rate as measured by satellite and different shallow and/or in-depth site-effect parameters. Indeed, if such a correlation is observed, it is then possible to use the large-scale map of the subsidence rate in Grenoble to retrieve a high-resolution map of a given site-effect parameter.

Multi-temporal Synthetic Aperture Radar Interferometry (InSAR) is an advanced remote sensing technique that has been proven indispensable in the study of the Earth's surface deformation (e.g., Doin et al., 2015; Zhu et al., 2022). It plays a crucial role in understanding and continuously monitoring subsidence phenomena, as it allows an exceptionally high level of precision in measuring subsidence rates, often down to millimeter-scale accuracy (e.g., Raspini et al., 2022). InSAR techniques also provide high density of measurements, especially in urban areas, relative to other different in-situ methodologies such as levelling, Ground Position System (GPS), GNSS or piezometers, etc, whose data are too scattered in space. Since the launch of the Sentinel-1 satellites in 2014, which are continuously providing images of the Earth's surface, multiple services have emerged to generate open-access InSAR time-series products covering extensive regions. Examples of these services include the ForM@Ter LArge-Scale Multi-Temporal Sentinel-1 InterferoMetry service (FLATSIM, Thollard et al., 2021) and the European Ground Motion Service (EGMS, Costantini et al., 2021). In this context, this study aims at investigating the correlation between subsidence rates in Grenoble and detailed maps of various site-effect parameters: V_{S10} (time-averaged shear waves velocity down to a depth of 10 m, V_{S30} is only available at a few points scattered throughout the basin), f_0 (fundamental resonance frequency of the soil), $\log_{10}(f_0)$, T_0 (period of resonance of the soil) and H_{bed} (bedrock depth). We present the different sets of available data and explain the methodology to compute the different correlations and the strategy to reach an acceptable level of regression. Results are finally discussed, and we conclude on different perspectives that could be achieved in future works.

2. Geophysical data available in the Grenoble basin and data smoothing in space

Grenoble, an alpine city located in southeastern France, constitutes a Y-shaped valley surrounded by three rock massifs: Vercors to the West, Chartreuse to the North and Belledonne to the South-East (Figure 1). It constitutes a deep sedimentary basin with bedrock going down to 900 m depth (Vallon, 2014). The filling of the valley was primarily controlled by two glacial-interglacial cycles (Riss-Würm and Holocene periods), followed by lacustrine sedimentation of homogeneous deposits (sandy or clayey silts), which were subsequently overlaid by heterogeneous alluviums from two rivers: the Drac (clay and silt sediments) and the Isère (gravels and sand sediments; Couturier, 1974). The Quaternary surface deposits exhibit two main units: gravel sediments spanning from the northwest to the center of the valley, surrounded by clayey sediments to the East and West (Figure 2). Grenoble is an active seismic region characterized by a relatively low-to-moderate level of earthquake activity. Its historical seismicity shows the potential for seismic events with a

magnitude reaching 5.5 in the vicinity of the city (Causse et al., 2009). The French seismic zoning assigns level 4 to Grenoble city (out of 5, 4 being the maximum in mainland France), which corresponds to a 10% probability of exceeding macroseismic intensity VIII at the rock sites within 50 years.

2.1. InSAR data and subsidence rates

The InSAR time-series data covering Grenoble between May 2016 and December 2021, was acquired for the Sentinel-1 descending track 139 from EGMS (Costantini et al., 2021). EGMS offers the Line Of Sight (LOS) displacement time-series from both ascending and descending Sentinel-1 satellite missions, encompassing the entire European region. The time-series is computed by incorporating all acquisitions from both Sentinel-1A and Sentinel-1B satellites, with an acquisition interval of one image every six days. EGMS utilizes the Advanced Differential Interferometric Synthetic Aperture Radar (A-DInSAR) technique, incorporating advanced persistent scatterer (PS) and distributed scatterer (DS) InSAR processing techniques along with a high-quality Global Navigation Satellite System (GNSS) model for ground-motion product calibration (see more details about the method in Crosetto et al., 2021; Costantini et al., 2021). The displacement time-series for Grenoble offers a reliable measurement of mean subsidence rate in LOS over four and a half years, distributed unevenly across the area, with points ranging from a few meters to a few kilometres apart, depending on the surface cover. The subsidence rates for Grenoble (Figure 1b) predominantly indicate an increase in velocities from the basin's edge towards its centre, with some velocities reaching up to 10 mm/yr LOS.

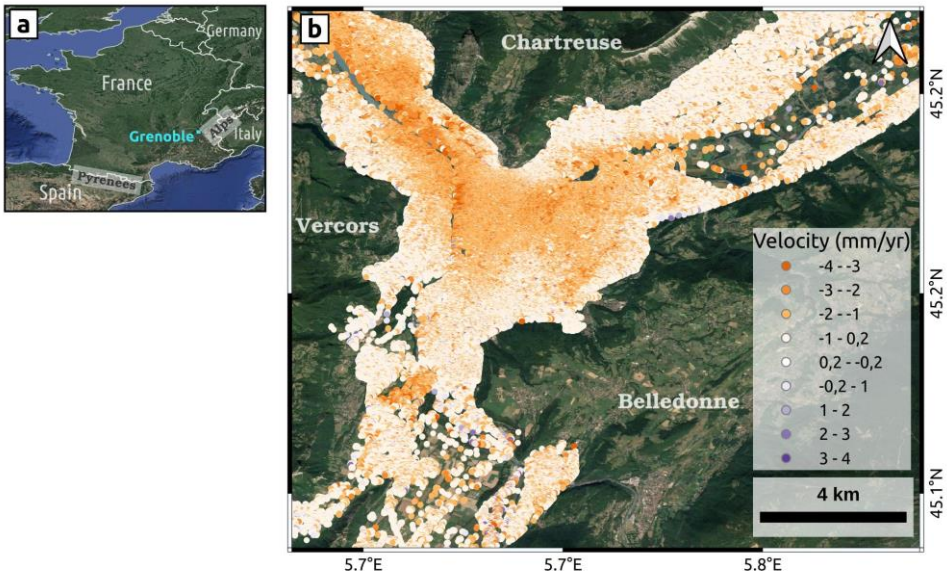

Figure 1. (a) Location map of Grenoble city in France. (b) InSAR LOS velocity measurements from EGMS, cropped over the Grenoble sedimentary basin. Negative values, shown in orange, indicate surface displacement away from the satellite (i.e., subsidence of the soil).

Because of the high local variability of the subsidence values, we apply a spatial averaging (smoothing) of the subsidence rate at different wavelengths to mitigate the effects of isolated extreme values. To achieve this, we calculate the median subsidence rate obtained at each point within a diameter varying from 100 m to 3000 m and centred on the considered point. By doing so, we smooth the data over different distances, reducing the spatial variability and reducing extreme values.

2.2. Shallow basin site-effect data

These data were obtained through single-point measurements of Multichannel Analysis of Surface Waves (MASW), which were then inverted in conjunction with geological information gathered from 100 boreholes in Grenoble. This process aimed to determine the velocity of various superficial sediment types, mainly gravels, clays, and sands (Cartier and Cornou, 2016). The resultant velocities for each sediment type were subsequently applied to all the boreholes in Grenoble to calculate their V_{S10} values (Figure 2).

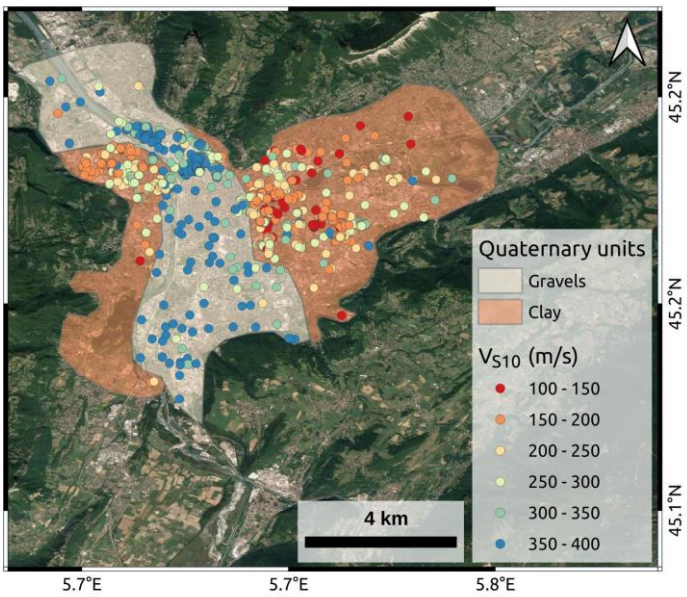

Figure 2. Map of V_{S10} (time-averaged shear waves velocity down to a depth of 10 m) measured in the Grenoble basin, showing the delineation of the clay and gravel Quaternary units.

2.3. In-depth basin site-effect data

The in-depth site-effect data available for the Grenoble basin consist of measurements of the fundamental resonance frequency and of the bedrock depth. The city is covered with 579 estimates of resonance period acquired from numerous campaigns of ambient-noise H/V measurements carried out between 1995 and 2009 (Scherbaum et al., 1999; Bettig et al, 2001; Lebrun et al., 2001; Cornou et al, 2003; Bonnefoy-Claudet, 2004; Chaljub et al., 2006; Hobiger, 2006; Guéguen et al., 2007). The sensors used in these studies were either medium-band velocimeters (Lennartz 5s, CMG40) or low-frequency amplified accelerometers. The resonance period measures are not evenly distributed in the area, the distance separating two points varies from few meters to kilometers (Figure 3).

The bedrock depth data were modelized from gravimetric measurement campaigns carried out between 1981 and 1999 by Vallon (2014). A total of 419 gravity measurement points is available in an area of 240 km² covering the Grenoble basin (316 stations) and extending into parts of the surrounding massifs (103 stations). The density of the stations is very variable, ranging from an average of 4.7 stations/km^2 in the basin (with a maximum of 9 stations/km^2) to 0.6 stations/km^2 on the hills. The bedrock depth model was then computed on a regular grid of 250 m (Figure 4). According to Vallon (2014), certain areas exhibit greater uncertainties in gravimetric measurements and corrections, with the accuracy of bedrock depth values being lower at the periphery of the basin compared to the central area. The high uncertainty on the hills and at the edges of the basin are related to the complexity of the topography and to the low number of gravimetric measures, in addition to the incorrect assumption that the alluvial filling of the plain has no gravitational effect beyond the plain itself, which is not the case (Vallon, 2014).The highest resonance periods in the center of the Grenoble valley (Figure 3) coincide with places where the bedrock is deepest (Figure 4). These high periods and bedrock depths correspond to an average V_S around 700 m.s^{-1} which is coherent with the geophysical informations.

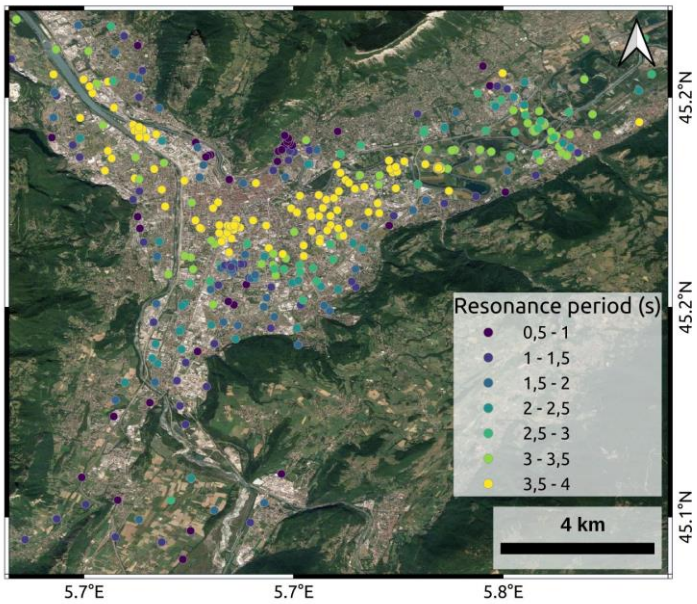

Figure 3. Map of site-effect resonance period measurements in the Grenoble basin.

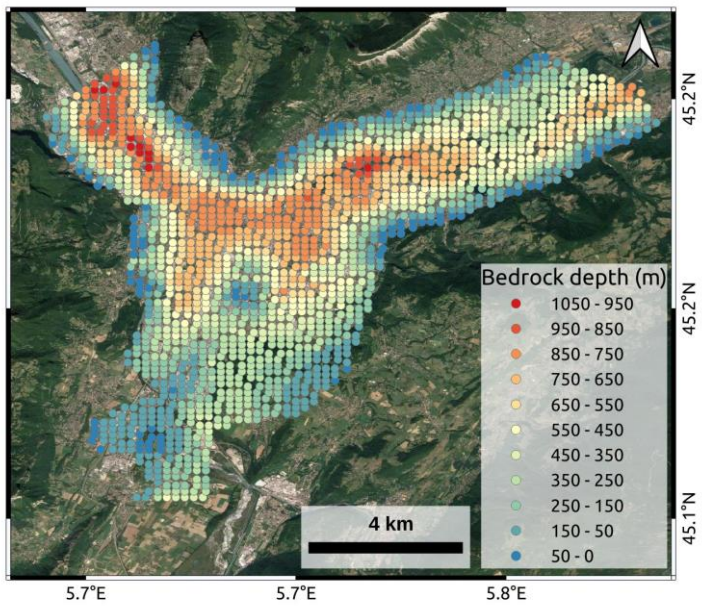

Figure 4. Map of bedrock depth below the Grenoble basin as modelized by Vallon (2014) from the inversion of gravimetric anomalies.

3. Linear correlations between subsidence rates in the Grenoble basin and site-response parameters

3.1. Methodology

The site-effect parameters investigated (V_{S10}, f_0, T_0, $\log_{10}(f_0)$ and H_{bed}) were obtained from punctual measures, with their own spatial resolutions. The subsidence rate is the input parameter to the analysed correlation, for which we have the higher spatial resolution. Therefore, to associate a subsidence rate beneath each site-effect measurement point, we consider the subsidence value that is closest in space. We then compute the linear correlation between the subsidence rate and each site-effect parameter one by one, using the Matlab Statistics and Machine Learning toolbox. We obtain a Coefficient of Determination R^2 that we compare for each correlation investigated. We explore the optimization of the correlation by smoothing the subsidence rate over different lengths, as explained in section 2.2.1. We investigate also the potential outliers that could reduce the

R^2 value. Table 1 summarises the R^2 values obtained for the different tested correlations, with and without outliers, and for different levels of smoothing on the subsidence rates. When looking at the evolution of the R^2 value as a function of the smoothing length applied on the subsidence rates to correlate them with the site-effect parameters (Figure 5), it appears that a particular length (870 m) allows to reach a R^2 maximum in all correlations. This length is therefore selected in the following.

Table 1. Values of regression coefficient R2 obtained in the linear regression of soil subsidence rates in the Grenoble basin with different targeted site-effect parameters, with and without including outliers, and with three different levels of smoothing of the subsidence rates.

Targeted parameter	**Outliers**	**Without smoothing**	**With smoothing length of 350 m**	**With smoothing length of 870 m**
Bedrock depth (H_{bed})	With	0.1198	0.3083	0.4388
	Without	0.2503	0.5547	0.6704
Fundamental resonance frequency (f_0)	With	0.0347	0.0873	0.1345
	Without	0.0665	0.1433	0.2220
$Log_{10}(f_0)$	With	0.0822	0.1730	0.2705
	Without	0.1276	0.2255	0.3534
Period of resonance (T_0)	With	0.1037	0.2100	0.3220
	Without	0.1662	0.3704	0.5265
V_{S10}	With	0.0163	0.0462	0.0384
	Without	0.0604	0.1592	0.1628

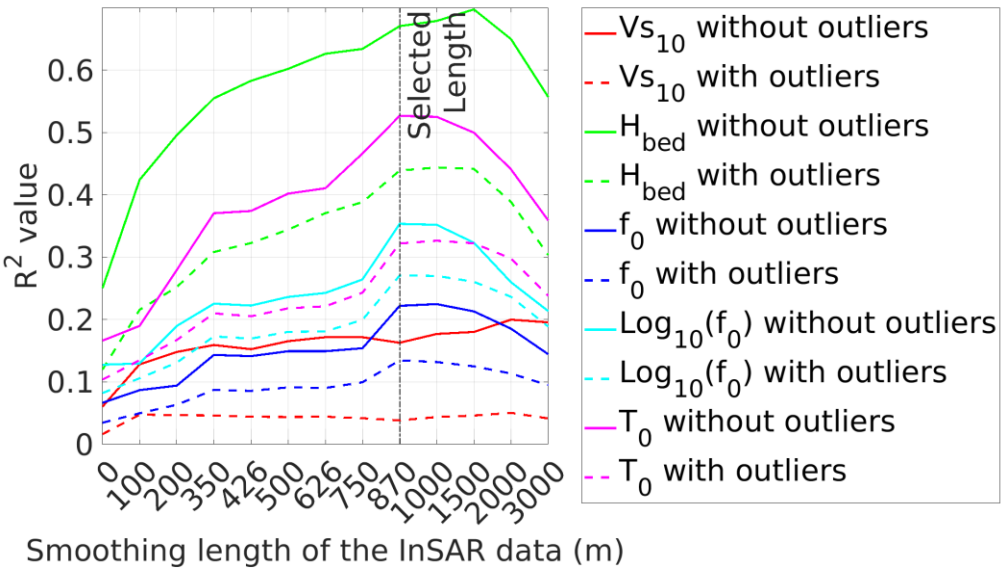

Figure 5. Values of regression coefficient R^2 as a function of the smoothing length of the subsidence rates from InSAR. Dotted lines are obtained when no outlier is removed from the dataset, solid lines are obtained when removing outliers. The black vertical line indicates the smoothing length selected for this study, at which almost all R^2 reach their maximal value.

3.2. Correlation of subsidence rates with a shallow site-effect parameter

The first parameter investigated is a site-effect parameter that represents the seismic response of the shallow soil. We investigate the correlation of the subsidence rates in the Grenoble valley with the time-averaged

shear-wave velocity in the top 10 meters of soil (V_{S10}) and the quaternary deposits (not shown in this study). Without smoothing the subsidence data, the R^2 value obtained for the correlation between the subsidence rate and V_{S10} is very low (R^2 = 0.0163). Even when adding smoothing and removing outliers, the R^2 value never exceeds 0.2. Those results support no correlation between the subsidence rates and V_{S10}, hence no clear correlation of the subsidence rates appears with the shallow part of the site effect in the Grenoble basin.

3.3. Correlation of subsidence rates with in-depth site-effect parameters

The second set of parameters investigated concerns parameters that represent the seismic response of the whole sedimentary column in the Grenoble basin. The first targeted parameter is the fundamental frequency of the soil (f_0). Without smoothing of the subsidence rates, the R^2 obtained is roughly of the same order as the one obtained previously for V_{S10}. However, by applying the selected smoothing of 870 m on the InSAR data, we increase the value of R^2 above 0.2 (see Table 1), which we interpret as a potential for a physical correlation between the two parameters, but that is not yet accurately expressed. Indeed, the linear correlation improves when using the logarithmic value of the frequency ($\log10(f_0)$), but the R^2 still does not exceed 0.3. A major improvement appears when considering the fundamental resonance expressed in period (T_0 in seconds) instead of frequency (f_0 in hertz). By doing so, we increase the value of R^2 above 0.3.

The histogram of the Pearson's residuals obtained for the linear correlation between T_0 and subsidence rates smoothed over the optimized length of 870 m is displayed in Figure 6a. Few residuals are below –1.5 or above 1.5. We assume these points to be potential outliers and we process again the linear regression by excluding them from the dataset. Figure 6b represents the linear function obtained over the scatter plot, with the excluded outliers circled in red. By excluding outliers and by smoothing the subsidence rates over a length of 870, the value of R^2 can exceed 0.5 (see Table 1). However, we need to demonstrate that excluding outliers is physically justified, which we do in section 3.3.4.

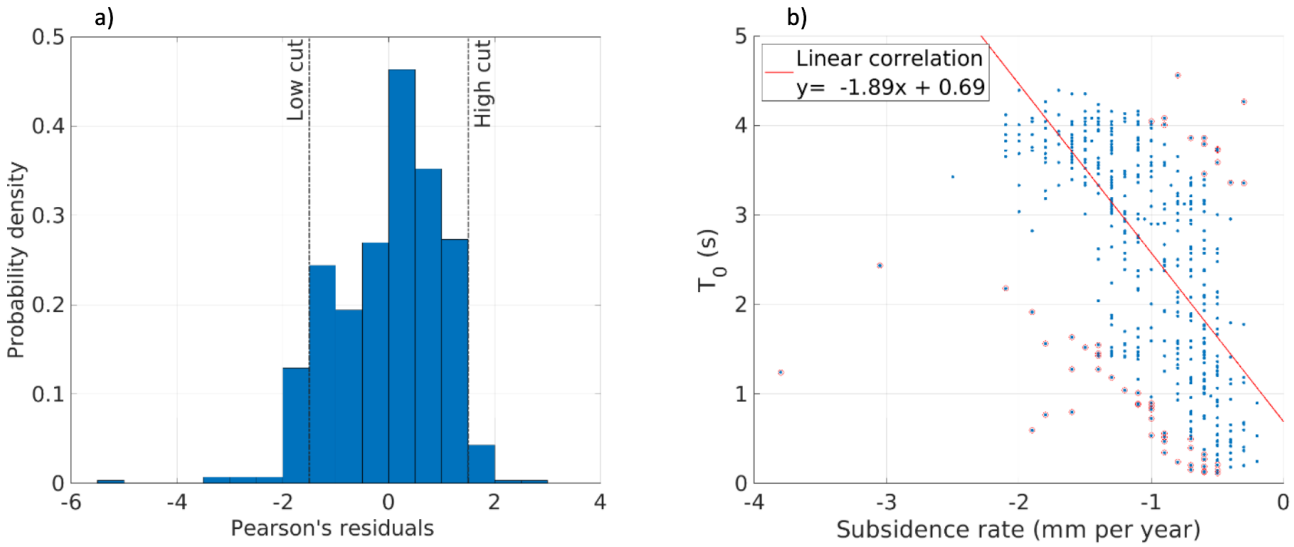

Figure 6. (a) Histogram of Pearson's residuals obtained in the linear regression of subsidence rates in the Grenoble basin with the resonance period T_0, and for a smoothing length of 870 m. (b) Scatter plot of the linear correlation between the subsidence rate and the resonance period (T_0) in the Grenoble basin. The red line represents the optimized linear function, and the red circled dots are outliers as defined in Figure 6a.

The last in-depth parameter that is tested is the bedrock depth (H_{bed}), by applying the same workflow than for T_0. The linear function obtained is shown in Figure 7, where the potential outliers in the correlation of subsidence rates with H_{bed} are marked by the red circles. Note that this linear correlation shows that for a subsidence rate close to 0 mm/yr the predicted bedrock depth is also 0 m, which is totally in accordance with what is to be expected, since the outcropping bedrock is not subsiding. The R^2 value obtained in that case reaches 0.67 (Table 1).

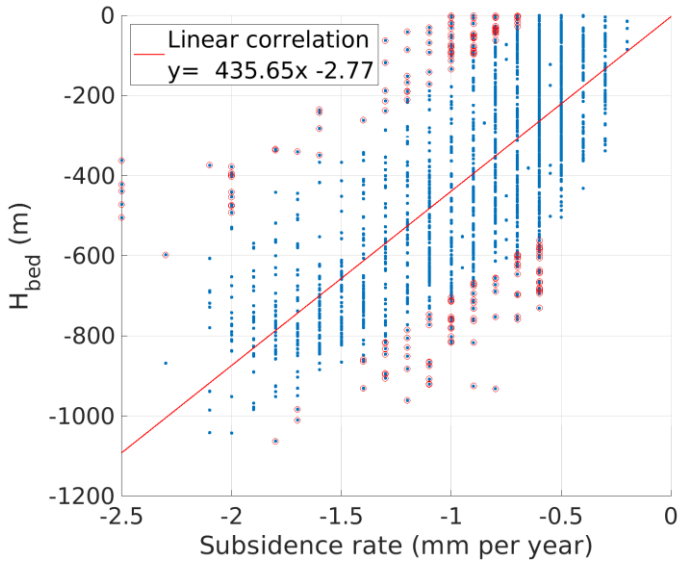

Figure 7: Scatter plot of the linear correlation between the subsidence rate and the bedrock depth in the Grenoble basin. The red line represents the optimized linear function, and the red circled dots are defined as potential outliers (see text).

Table 2 shows the evolution of the two coefficients p (intercept) and m (slope) of the linear function obtained after linear regression between subsidence rates and H_{bed}/T_0, as a function of the level of smoothing on the subsidence rates. The coefficients of the equation vary greatly depending on the smoothing level, which emphasizes the need to determine the quantity of smoothing adequate to retrieve a physical correlation. In our case study, for the bedrock depth, the intercept p clearly tends towards 0 for a smoothing length around 870 m - 1000 m, which makes physical sense. The same effect is awaited with T_0, which is the case, although less blatantly, for a smoothing length between 870 m – 1500 m.

Table 2. Coefficient (slope) and intercept of the linear-regression function obtained for the bedrock depth and the period when correlated with the subsidence rates in the Grenoble basin.

	Bedrock depth H_{bed}		**Period T_0**	
	p (intercept)	m (slope)	p (intercept)	m (slope)
No smoothing	-244.61	122.67	2.24	-0.44
Smoothing 100 m	-150.05	242.76	2.07	-0.58
Smoothing 750 m	-20.34	412.86	0.92	-1.70
Smoothing 870 m	-2.77	435.65	0.69	-1.89
Smoothing 1000 m	-0.18	440.47	0.71	-1.89
Smoothing 1500 m	26.44	476.40	0.65	-1.99
Smoothing 2000 m	31.27	482.45	0.75	-1.94
Smoothing 3000 m	49.38	490.53	0.84	-1.88

3.4. Potential origins of outliers in the linear correlation between subsidence rates and site-effect parameters in the Grenoble basin

As explained in the previous section, the correlations are improved by excluding the most extreme points that less follow the linear correlation of the site-effect parameters with the subsidence rates. To have a better understanding of what could be the physical origins of these outliers, we map all the outliers of the T_0 and H_{bed}

correlations in Figure 8 to observe whether they have a random or specific location in the basin. It appears that for a large majority of outliers, their location is not random, and they group together in clusters. We identify 5 potential origins of the outliers, numbered from 1 to 5 in Figure 8, and listed hereafter:

1. Location close to the edges of the basin; As the subsidence rate is very low, it may not be measured by InSAR with a good accuracy, or the measure of f_0 is less accurate due to 3D effects (Guéguen et al., 2007), or the accuracy of bedrock depth values is lower at the periphery of the basin compared to the central area (Vallon 2014).
2. Area with heavy buildings (*Base de données nationale des bâtiments* BDNB - data.gouv.fr), that can cause an overestimation of the subsidence rate in the investigated time frame.
3. Irregular or complex bedrock geometry at depth; as a result, the geometry is not 1D and the measure of f_0 may be biased.
4. Area corresponding to strong and variable gravimetric anomalies (Vallon 2014) that cause the bedrock depth model to be less constrained.
5. The distance between the site-effect parameter and the closest InSAR point is too large (> 200 m).

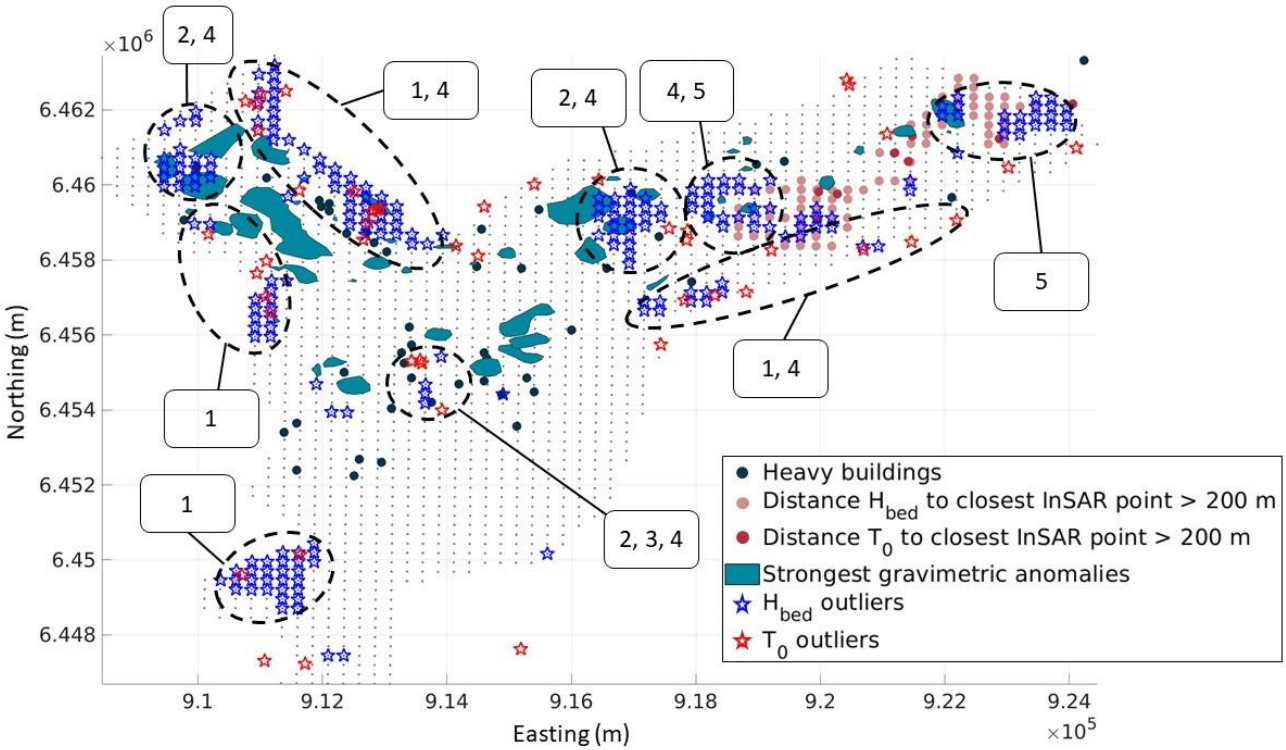

Figure 8. Interpreted map of the outliers in the linear regression between subsidence rates and bedrock depths (blue stars) or resonance periods (red stars) in the Grenoble basin. The potential origins of the clusters of outliers are indicated by the colored dots and by the numbered labels (see text).

4. Conclusions and perspectives

We investigate in Grenoble, a well-studied sedimentary basin prone to strong site effects, the correlation between the subsidence rate of the sediments as measured by InSAR and 5 physical parameters of the site response: V_{S10}, f_0, T_0, $\log_{10}(f_0)$ and H_{bed}. While we find no correlation with the surface parameter V_{S10}, we find an acceptable linear correlation (R^2 larger than 0.5) for some of the in-depth site parameters. The best linear fits are obtained with the bedrock depth (R^2 =0.67) and the resonance period (R^2 = 0.53). As the bedrock depth increases, the thickness of the sedimentary soil column increases as well, and the settling of the soil due to its own weight increases too, hence the subsidence rate is higher. The correlation is improved when using the logarithmic value of the frequency (instead of f_0), but mostly by smoothing the subsidence rates over a particular spatial extent that we determine to be optimal at 870 m. By doing so, we reduce the spatial variability and the extreme values of the subsidence rates.

Another improvement is brought by excluding outliers from the dataset of H_{bed} and T_0 values, that we interpret as values that are affected by high uncertainties. We explore the origins of those potential outliers. Their

location in the Grenoble basin is not aleatory and they tend to group into clusters. Most of the outliers can be explained by physical processes or by uncertainties on the measurement methods. In total, we suggest 5 potentials origins for the outliers. For example, a large part of the outliers is found on the edges of the basin, where the very slow subsidence rate may not be measured with enough accuracy, and where the slope of the bedrock below the sediments may also false the f_0/T_0 measure. Other outliers can be explained by the lack of a close InSAR measurement point, presence of heavy building nearby, or uncertainty in the model of the bedrock depth.

The linear equations derived in this study are valid only for the Grenoble basin. We should explore such correlations in several other valleys, that may present different values of subsidence rate, bedrock depth and resonance period, to better understand the physics of these correlations, and in particular the physical meaning of the coefficient and intercept of the equations obtained. The analysis of the origins of the outliers must be deepened, in order to determine if it is possible to correct some outlier values and to keep them on the dataset. The correlations obtained will allows to map the bedrock depth and the fundamental period of resonance in the Grenoble basin at a finer spatial resolution. As a future work, we will test different correlations with multiple inputs, for example in associating a velocity model with the subsidence rate to be able to forecast the levels of amplification. These levels of amplification, obtained at a fine scale, could then be used as an input in the shakemaps to retrieve a high-resolution map of intensity.

5. Acknowledgments

This study is supported by a public grant overseen by the French National Research Agency (ANR) through the project SASHA (Grant Number ANR-22-CE04-0013).

6. References

Allen, T.I. and Wald, D.J. (2009) 'On the Use of High-Resolution Topographic Data as a Proxy for Seismic Site Conditions (VS30)', *Bulletin of the Seismological Society of America*, 99(2A), pp. 935–943. Available at: https://doi.org/10.1785/0120080255.

Bard, P.-Y. *et al.* (1988) 'The Mexico Earthquake of September 19, 1985—A Theoretical Investigation of Large- and Small-scale Amplification Effects in the Mexico City Valley', *Earthquake Spectra*, 4(3), pp. 609–633. Available at: https://doi.org/10.1193/1.1585493.

Base de données nationale des bâtiments (BDNB) - data.gouv.fr (2023). Available at: https://www.data.gouv.fr/fr/datasets/base-de-donnees-nationale-des-batiments/ (Accessed: 11 October 2023).

Bettig B., Bard, P.-Y., Scherbaum, F., Riepl, J., Cotton, F., Cornou, C., and Hatzfeld, D. (2001). Analysis of dense array noise measurements using the modified spatial auto-correlation method (SPAC): application to the Grenoble area. Bolettino di Geofisica Teorica ed Applicata; 42(3-4), 281-304.

Bonnefoy-Claudet, S. (2004) *Nature du bruit de fond sismique: implications pour les études des effets de site*. PhD Thesis. University Joseph Fourier, Grenoble, France. Available at: https://theses.hal.science/tel-00007397.

Cadet, H. (2008) 'A New proposal for site classification based on ambient vibration measurements and the kiknet strong motion data set', in. *The 14th World Conference on Earthquake Engineering*, Beijing, China. Available at: https://www.iitk.ac.in/nicee/wcee/article/14_03-01-0036.PDF.

Cartier, S. and Cornou, C. (2016) 'New soil information and financial scenarios to promote earthquake-resistance in the school buildings of Grenoble area', in *Faire face aux risques dans les sociétés contemporaines*. Octares editions. (Collection Le travail en débat).

Causse, M. *et al.* (2009) 'New approach for coupling k^{-2} and empirical Green's functions: application to the blind prediction of broad-band ground motion in the Grenoble basin', *Geophysical Journal International*, 179(3), pp. 1627–1644. Available at: https://doi.org/10.1111/j.1365-246X.2009.04354.x.

Chaljub, E., Cornou, C., Verbeke, J., Converset, J., Voisin, C., Stehly, L., Grasso, J.-R., Guéguen, P., Roussel, S., Roux, P., Hatton, S. and Campillo, M. (2006). Measurement and variability study of site effects in the 3D glacial valley of Grenoble, French Alps. Proc. 3nd Int. Symp. on the Effects of Surface Geology on Seismic Motion, Grenoble, 30 August - 01 September, 2006, Bard, P.Y., Chaljub, E., Cornou, C., Cotton, F. and Guéguen, P. Editors, LCPC Editions, paper# 154

Cornou, C. (2003) 'Contribution of Dense Array Analysis to the Identification and Quantification of Basin-Edge-Induced Waves, Part II: Application to Grenoble Basin (French Alps)', *Bulletin of the Seismological Society of America*, 93(6), pp. 2624–2648. Available at: https://doi.org/10.1785/0120020140.

Costantini, M. *et al.* (2021) 'European Ground Motion Service (EGMS)', in *2021 IEEE International Geoscience and Remote Sensing Symposium IGARSS*. *2021 IEEE International Geoscience and Remote Sensing Symposium IGARSS*, pp. 3293–3296. Available at: https://doi.org/10.1109/IGARSS47720.2021.9553562.

Couturier, B. (1974) *Contribution à l'étude géologique, hydrogéologique et géotechnique du bas Grésivaudan (Isère)*. PhD Thesis. University Grenoble Alpes, Grenoble, France. Available at: https://theses.hal.science/tel-00614816/.

Crosetto, M. *et al.* (2021) 'Deformation monitoring at european scale: the copernicus ground motion service', *The International Archives of the Photogrammetry, Remote Sensing and Spatial Information Sciences*, XLIII-B3-2021, pp. 141–146. Available at: https://doi.org/10.5194/isprs-archives-XLIII-B3-2021-141-2021.

Cultrera, G. *et al.* (2021) 'Indicators for site characterization at seismic station: recommendation from a dedicated survey', *Bulletin of Earthquake Engineering*, 19(11), pp. 4171–4195. Available at: https://doi.org/10.1007/s10518-021-01136-7.

Doin, M.-P. *et al.* (2015) 'InSAR measurement of the deformation around Siling Co Lake: Inferences on the lower crust viscosity in central Tibet', *Journal of Geophysical Research: Solid Earth*, 120(7), pp. 5290–5310. Available at: https://doi.org/10.1002/2014JB011768.

European Commission. Joint Research Centre. (2012) *Eurocode 8: seismic design of buildings Worked examples.* LU: Publications Office. Available at: https://data.europa.eu/doi/10.2788/91658 (Accessed: 27 September 2023).

Frankel, A.D. (2002) 'Nonlinear and Linear Site Response and Basin Effects in Seattle for the M 6.8 Nisqually, Washington, Earthquake', *Bulletin of the Seismological Society of America*, 92(6), pp. 2090–2109. Available at: https://doi.org/10.1785/0120010254.

Graves, R.W., Pitarka, A. and Somerville, P.G. (1998) 'Ground-motion amplification in the Santa Monica area: Effects of shallow basin-edge structure', *Bulletin of the Seismological Society of America*, 88(5), pp. 1224–1242. Available at: https://doi.org/10.1785/BSSA0880051224.

Guéguen, P. *et al.* (2007) 'On the Limitation of the H/V Spectral Ratio Using Seismic Noise as an Exploration Tool: Application to the Grenoble Valley (France), a Small Apex Ratio Basin', *Pure and Applied Geophysics*, 164(1), pp. 115–134. Available at: https://doi.org/10.1007/s00024-006-0151-x.

Hobiger, M. (2006) *Caractérisation expérimentale et numérique des résonances globales de la vallée grenobloise*. Master's thesis report. University Joseph Fourier, Grenoble, France.

Lebrun, Beno., Hatzfeld, D. and Bard, P.Y. (2001) 'Site Effect Study in Urban Area: Experimental Results in Grenoble (France)', *Pure and Applied Geophysics* [Preprint]. Available at: https://doi.org/10.1007/978-3-0348-8177-7_16.

Luzi, L. *et al.* (2011) 'Proposal for a soil classification based on parameters alternative or complementary to Vs,30', *Bulletin of Earthquake Engineering*, 9(6), pp. 1877–1898. Available at: https://doi.org/10.1007/s10518-011-9274-2.

Michel, S. *et al.* (2011) 'May subsidence rate serve as proxy for site effects?', in *Poster contribution to SSA's 2010*. *Seismological Society of America*, Portland, United States. Available at: https://www.researchgate.net/publication/280858317_May_subsidence_rate_serve_as_proxy_for_site_effects.

Pratt, T.L. (2003) 'Amplification of Seismic Waves by the Seattle Basin, Washington State', *Bulletin of the Seismological Society of America*, 93(2), pp. 533–545. Available at: https://doi.org/10.1785/0120010292.

Raspini, F. *et al.* (2022) 'Review of satellite radar interferometry for subsidence analysis', *Earth-Science Reviews*, 235, p. 104239. Available at: https://doi.org/10.1016/j.earscirev.2022.104239.

Scherbaum, F., Riepl, J., Bettig, B., Ohrnberger, M., Cornou, C., Cotton, F. and Bard, P.-Y. (1999). Dense array measurements of ambient vibrations in the Grenoble basin to study local site effects, AGU Fall meeting, San Francisco, December 1999.

Thollard, F. *et al.* (2021) 'FLATSIM: The ForM@Ter LArge-Scale Multi-Temporal Sentinel-1 InterferoMetry Service', *Remote Sensing*, 13(18), p. 3734. Available at: https://doi.org/10.3390/rs13183734.

Vallon, M. (2014) *Estimation de l'épaisseur d'alluvions quaternaires dans la cuvette grenobloise par inversion des anomalies gravimétriques.*, p. 37. Available at: https://insu.hal.science/insu-01060584.

Wald, D.J. and Allen, T.I. (2007) 'Topographic Slope as a Proxy for Seismic Site Conditions and Amplification', *Bulletin of the Seismological Society of America*, 97(5), pp. 1379–1395. Available at: https://doi.org/10.1785/0120060267.

Wald, D.J. *et al.* (1999) 'TriNet "ShakeMaps": Rapid Generation of Peak Ground Motion and Intensity Maps for Earthquakes in Southern California', *Earthquake Spectra*, 15(3), pp. 537–555. Available at: https://doi.org/10.1193/1.1586057.

Worden, C.B. *et al.* (2010) 'A Revised Ground-Motion and Intensity Interpolation Scheme for ShakeMap', *Bulletin of the Seismological Society of America*, 100(6), pp. 3083–3096. Available at: https://doi.org/10.1785/0120100101.

Worden, C.B. *et al.* (2020) *ShakeMap 4 Manual — ShakeMap Documentation documentation, ShakeMap Manual Online: technical manual, user's guide, and software guide, U. S. Geological Survey.* Available at: http://usgs.github.io/shakemap/index.html (Accessed: 13 October 2023).

Zhu, C. *et al.* (2022) 'Time Series Multi-Sensors of Interferometry Synthetic Aperture Radar for Monitoring Ground Deformation', *Frontiers in Environmental Science*, 10, p. 929958. Available at: https://doi.org/10.3389/fenvs.2022.929958.